

Compact, fast multi-wavelength switchable single frequency laser

Christophe Moser, Lawrence Ho, Frank Havermeyer
Ondax, Inc., 850 E. Duarte Road, Monrovia, CA, USA 91016

ABSTRACT

We have developed a fast multi-wavelengths switching laser platform. The tuning mechanism is based on a micro-mirror array DLP chip from a commercial pico-projector forming the end mirror of an external cavity laser diode. We report progress on a working prototype of a single frequency laser with a wavelength that is switchable between any five wavelengths spanning 765 nm to 783 nm. Switching time between any two wavelengths is equal to the switching time of the DLP micro-mirrors (milliseconds). We show that there is a clear path to realizing a tunable laser with over 50 discrete wavelengths. In addition to the fast switching time between any wavelengths, this laser has a compact form factor ($<1\text{cm}^2$) and the design is applicable to a broad spectral range spanning 400 nm to 3,000 nm.

Keywords: fast, tunable lasers, micro-mirror, DLP, LCD, volume holographic grating

INTRODUCTION

A self-aligned external cavity diode laser based on volume holographic grating technology was recently introduced [1, 2]. The principle of the self-aligned cavity is illustrated in figure 1(a).

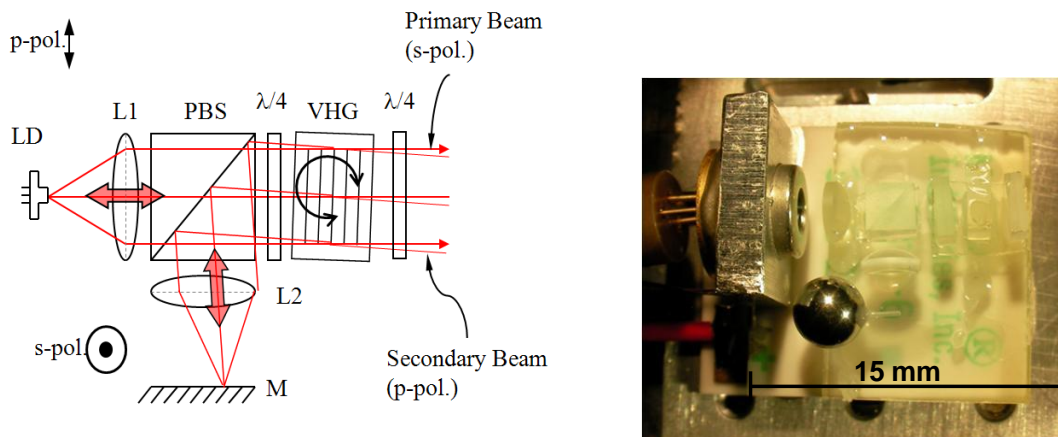


Figure 1: (a) Architecture of the self-aligned external cavity laser. (b) Picture of a prototype single frequency laser at 780 nm.

The p-polarized beam from the laser diode **LD** is collimated by lens **L1** and propagates through the polarizing beam splitter **PBS**. The reflective volume holographic grating **VHG** diffracts the beam. The diffracted beam is s-polarized after a double pass through the quarter waveplate $\lambda/4$. The diffracted s-polarized beam is reflected by the **PBS** towards a second lens **L2** which focuses the beam onto a highly reflective mirror **M** placed at the focal plane of lens **L2**. The back facet of the laser diode **LD** and the mirror **M** forms the resonant cavity. The mirror **M** retro-reflects the beam onto itself. The beam is re-collimated by lens **L2**, reflected by the **PBS** and incident on the **VHG** at precisely the same angle it was first diffracted. This produces a second diffracted beam which is exactly counter-propagating with the initial collimated beam. A second pass through the quarter waveplate $\lambda/4$ restores the polarization to p which is transmitted through the **PBS** and onto the laser diode facet. This resonant cavity is self-aligned because it is independent on the spatial and

angular position of the wavelength selective element (i.e. VHG). The external cavity laser diode (ECDL) wavelength is tunable by changing the angle of the VHG. The tuning range with this method is limited to a few nanometers.

Figure 1(b) shows a picture of the ECDL with all components mounted on a thermo-electric cooler.

2. Fast wavelength switching

An additional mechanism to increase the wavelength tuning range was proposed in [1, 2] but not experimentally demonstrated. Figure 2 illustrates the mechanism. There are two essential differences between figure 1 and figure 2 (1) a micro-mirror array **DLP** (or Liquid Crystal array **LCD**) replaces the mirror **M** shown in figure 1(a) (2) a **multiline VHG** replaces the single line VHG. The multiple distinct wavelengths diffracted by the **multi-line VHG** are brought to the focal plane of lens **L2**, where each beam's focus is physically separated (each beam corresponds to one distinct wavelength). Wavelength switching is achieved by switching the appropriate micro-mirror pixels or by rotating by 90 degrees the polarization of the appropriate LCD pixels. By appropriately selecting and switching the pixels, all but one diffracted beam is able to oscillate without loss in the external cavity and sustain lasing action while other beams are suppressed.

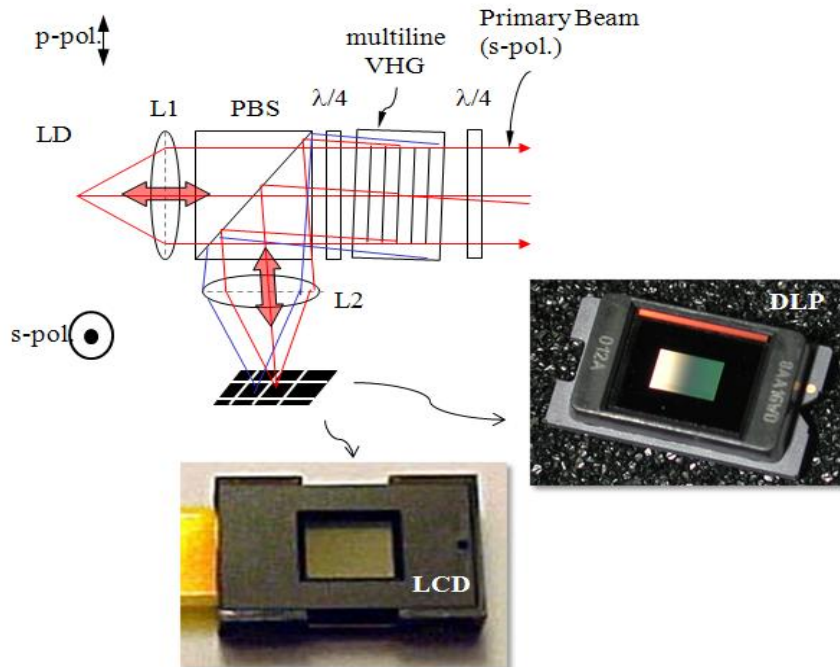


Figure 2: Schematic of the wavelength tuning architecture of the laser

3. Prototype laser

A prototype tunable laser following the illustration of figure 2 has now been implemented. Section 3.1 discusses the manufacturing and performance of the multiplexed VHG element and section 3.2 discusses the experimental results of the tunable laser.

3.1 Multiplexed volume holographic grating

A multiplexed VHG is a single physical element VHG containing multiple volume gratings within its volume. Following figure 2, the multiple wavelengths diffracted from the VHG are angularly separated. By recording each grating vectors

with distinct amplitude and direction, the wavelength diffracted and the angle of diffraction for that wavelength are unique.

The holographic recording method is illustrated in figure 3. The amplitude and direction of each grating vector can be selected by varying the angle of incidence of the reference and signal beam. The recording is performed sequentially, i.e one volume grating at a time.

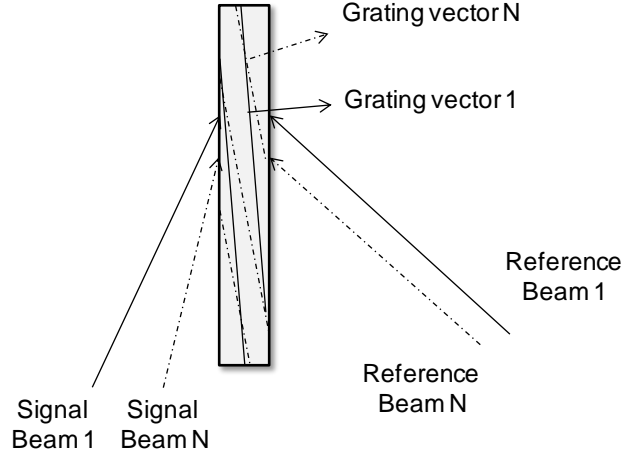


Figure 3: Sequential recording with pairs of reference and signal beam.

A 5x5x3 mm VHG with five multiplexed gratings with specific target wavelength and slant angle was recorded (the slant angle is the angle between the grating vector and the normal to the front facet of the VHG). The multiplexed VHG was then measured [3]. Table 1 shows the measured performance of the fabricated multiplexed VHG compared with the target specification.

VHG Parameter at 23°C	Target	Measured
Grating #1		
λ_1 :Wavelength [nm]	785.0	785.15
Efficiency [%]	30	27
Grating #2		
Wavelength [nm]	$\lambda_1 - 0.14$	$\lambda_1 - 0.15$
Efficiency [%]	30	28
Grating #3		
Wavelength [nm]	$\lambda_1 - 1.8$	$\lambda_1 - 1.7$
Efficiency [%]	30	29
Grating #4		
Wavelength [nm]	$\lambda_1 - 15$	$\lambda_1 - 15.05$
Efficiency [%]	30	30
Grating #5		
Wavelength [nm]	$\lambda_1 - 20$	$\lambda_1 - 19.95$
Efficiency [%]	30	30

Table 1: Performance of a 5-lines multiplexed VHG.

Based on the test results in Table 1, the mean of the deviation between the target and actual measured values of the slant angle is 0.018 degrees and 72 pm for the wavelength. The relative wavelength accuracy between the first grating wavelength and subsequent grating wavelengths is 50 pm for wavelengths separated by tens of nanometers. The efficiency uniformity on the multiplexed gratings was excellent with a maximum efficiency variation of 3%.

3.2 Tunable laser performance

A micro-mirror array DLP from Texas Instruments (DLP is a registered Trade mark from Texas Instruments, see figure 2) was positioned at the back focal plane of the lens L2. The micro-mirror array has 480x320 pixels with size 7.5 x 7.5 μm .

The laser diode has a front facet reflectivity of 10^{-4} and a gain spectrum spanning 760 nm to 785 nm.

The DLP chip has a protective 0.5 mm thick window that seals the micro-mirrors. The focal lens of lens L2 was greater than the focal lens of collimating lens L1 in order to increase the depth of focus and obtain enough clearance in the back focal plane to position the DLP. The arrangement is shown in figure 4. When the DLP is powered off, the micro-mirrors are all parallel to the protective window. We measured the reflectivity of the micro-mirrors to be approximately 60% at 780 nm (incl. Fresnel reflection from the cover window).

The ECDL was lasing very reliably on the multiple wavelengths given by the multilines gratings (bottom left graph, figure 3). The three lasing wavelengths were measured with an EXFO spectrum analyzer with 1 pm accuracy. The two additional lines corresponding to 785.15 nm and 785.0 nm were not lasing simultaneously. We attribute this to mode competition dominated by the 783.5 nm line.

The lasing wavelength 770.092 nm is within 8 pm of the corresponding measured wavelength of grating #4 (770.10 nm). The lasing wavelength 765.469 nm is within 269 pm of the corresponding measured wavelength of grating #5 (765.20 nm). The lasing wavelength 783.535 nm is within 85 pm of the corresponding measured wavelength of grating #5 (783.45 nm).

The ECDL was single frequency at any one time and hopping between the three wavelengths. Single frequency operation was verified with a Fabry-Perot analyzer with 1.5 GHz free spectral range (bottom right graph, figure 4). Upon powering on the DLP with a uniform white image, all mirrors move from their rest position to +12 degrees. The micro-mirrors angle change was enough to induce a large loss in the cavity and prevent lasing on all wavelengths, thereby demonstrating the basic principle for a broad wavelength switchable ECDL.

The next step is to design the algorithm to find and switch the mirrors on which the light coming from each diffracted beam is focused.

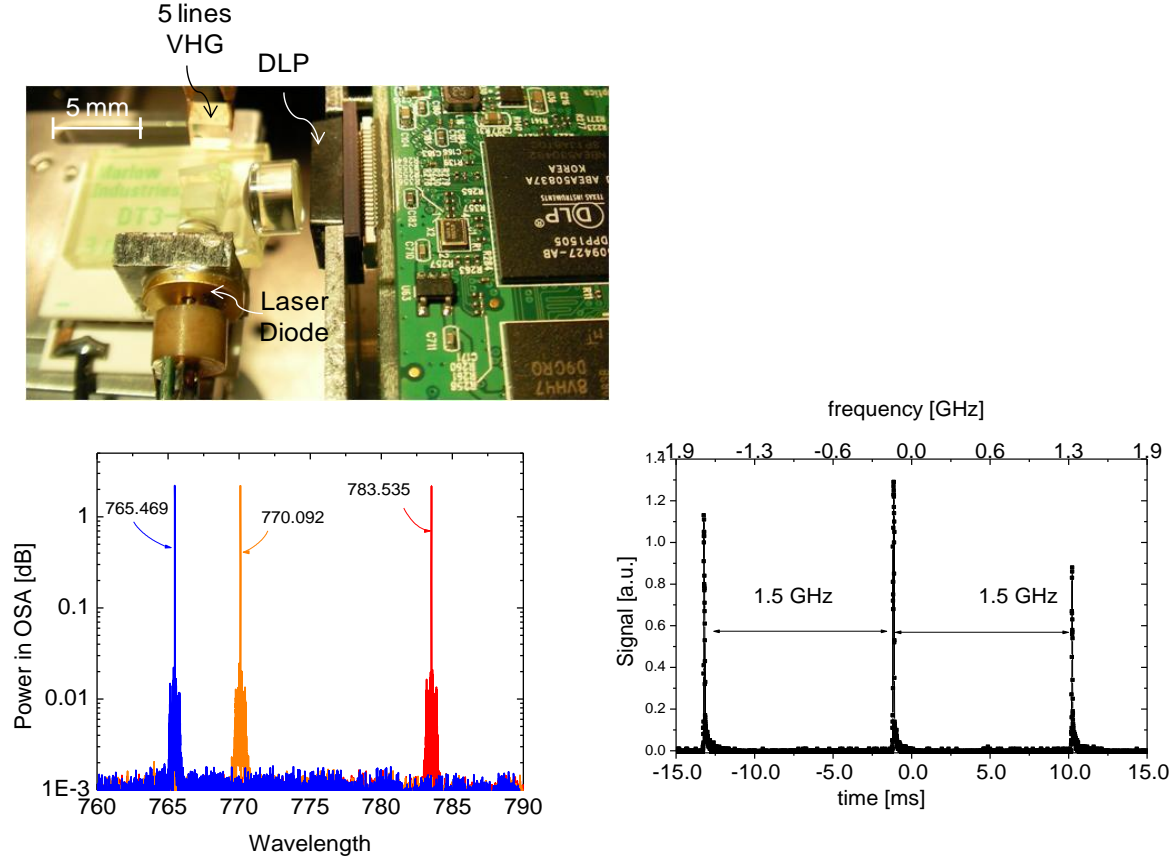


Figure 4: (top) picture of the prototype ECLD with a DLP mirror array as the wavelength tuning (switch) element and the 5-line multiplexed VHG. Three of the five lines are lasing simultaneously with the DLP array powered off (all mirrors facets in the plane of the focal plane). The lines disappear when the DLP is powered on.

The number of switchable wavelengths is equal to the number of multiplexed gratings. In section 4, we estimate the number of multiplexed gratings that can be recorded in a single element VHG.

4. Pushing the laser capability

The factor limiting the number of multiplexed gratings that can be recorded is the diffraction efficiency of each grating. As we show in the analysis below, the maximum refractive index contrast and the grating length determine the maximum amount of multiplexed gratings and thus the maximum number of switchable wavelengths in the laser.

The benefit of using the reflection holographic recording geometry is that a whole wafer can be recorded and tested with the automated testing stations available at Ondax, yielding hundreds of low-cost usable VHGs per wafers. The modulation depth (index contrast) of each individual grating recorded sequentially is:

$$m^{seq} = \frac{2\sqrt{r}}{N(1+r)}$$

where N is the number of multiplexed gratings and r is the intensity ratio between the signal and reference plane wave beams $r = I_S / I_R$.

This expression is maximized for $r=1$ (equal intensity between recording beams) $m_{\max}^{seq} = \frac{1}{N}$.

For a thick phase reflection grating, the diffraction efficiency η is given by [4]:

$$\eta = \tanh^2\left(\frac{\pi \cdot \Delta n \cdot L}{\lambda}\right), \quad (\text{equ 1.})$$

where L is the thickness (interaction length) of the grating, Δn the index of refraction modulation and λ the wavelength of the probe beam.

Let us perform an estimate at 785 nm, where the maximum index of refraction change that provide better than 90% transmission is approximately Δn_{\max} of $8 \cdot 10^{-4}$. This value is smaller than the maximum saturation refractive index change of the glass holographic material which is approximately $1.3 \cdot 10^{-3}$. Under this condition we can assume that the local refractive index change is proportional to the local light intensity. The modulation degree of the intensity pattern m^{seq} is therefore equal to the modulation degrees of the refractive index patterns.

A tunable laser at 785 nm requires a minimum grating thickness of approximately 3 mm in order to obtain the required narrow filter width. The grating efficiency used in the prototype laser was between 27% and 30%. Let us assume that an efficiency of 25% provides adequate feedback for the laser. The required index of refraction modulation can be computed from equ. 1 by setting $L=3$ mm and $\eta = 25\%$: $\Delta n_{req} = 4.6 \cdot 10^{-5}$.

Thus, the expected maximum number of multiplexed gratings with 25% efficiency is:

$$N = \frac{\Delta n_{\max}}{\Delta n_{req}} = 17.$$

By scaling the length L of the grating, the number of lines can be further increased. For example a VHG with 5 mm length provides 29 multiplexed gratings and a 10 mm long VHG provides 58 multiplexed gratings, each with 25% efficiency. Further tests on the required efficiency for adequate feedback is required. For example, if 15% efficiency is sufficient for each grating, a total of 78 multiplexed gratings can be recorded in one VHG 10 mm long.

5. CONCLUSIONS

A concept prototype single frequency laser with 5 switchable wavelengths in a footprint of 1.5 cm^2 has been shown and successfully demonstrated. A commercial DLP micro-mirror chip was used for the switching element and a VHG with five multiplexed grating to generate the 5 wavelengths. The concept can also be implemented with a commercial LCD chip. The unique aspect of the multi-wavelengths switchable laser platform is its small size, no moving parts and applicability to a spectral range from 400 nm to 3,000 nm.

Such combination of unique aspects are specially very attractive for applications using multi-wavelength interferometry [5], wavelength correction in holographic data storage [6], multi-wavelength vibrational microscopy [7], compact tunable terahertz sources [8] and bio-medical imaging [9].

This work has been supported by a phase I SBIR grant # 0839258 from the National Science Foundation.

REFERENCES

- [1] Moser, C., Ho, L. and Havermeier, F., "Self-aligned non-dispersive external cavity tunable laser" Optics Express, 16(21), pp.16691-16696 (2008).
- [2] Moser, C., Ho, L. and Havermeier, F., "A novel tunable diode laser using volume holographic gratings" Proceedings of the SPIE, Volume 7193, pp. 71930V-71930V-7 (2009).

- [3] Steckman, G., Havermeier, F., "High spatial resolution measurement of volume holographic gratings," Proceedings of the SPIE, Volume 6136, pp. 613602.1-613602.9 (2006).
- [4] Goodman, J., "Introduction to Fourier Optics," 2nd edition, Mc-Graw-Hill (1996).
- [5] Aleksoff, C., "Multi-Wavelength digital holographic metrology," Proceedings of the SPIE, Volume 6311, pp. 63111D.1-63111D.7 (2006).
- [6] Toishi, M., Tanaka, T., Sugiki, M., Watanabe, K., "Improvement in temperature tolerance of holographic data storage using wavelength tunable laser", Japanese Journal of Applied Physics, 45, pp. 1297-1304 (2006).
- [7] Knoll, B., Keilman, F., "Near-field probing of vibrational absorption for chemical microscopy", Nature, 399 (6732), pp 134-137 (1999).
- [8] Shi, W., Ding, Y., Fernelius, N., Vodopyanov, K., "Efficient tunable and coherent 0.18 -5.27 THz source based on GaSe crystal", Optics Letters, 27 (16), pp. 1454-1456 (2002).
- [9] Razansky, D., Distel, M., Vinegoni, C., Ma, R., Perrimon, R., Koster, R. & Ntziachristos, V., "Multi-spectral opto-acoustic tomography of deep seated fluorescent proteins in vivo", Nature Photonics, 3, pp. 412-417 (2009).